

DOI: 10.1002/cplu.201100008

Fabrication of Soft Submicrospheres by Sequential Boronate Esterification and Their Dynamic Behavior

Ryuhei Nishiyabu, Shiori Teraoka, Yusuke Matsushima, and Yuji Kubo*^[a]

Pyridine-assisted sequential boronate esterification of benzene-1,4-diboronic acid and 1,2,4,5-tetrahydroxybenzene has induced hierarchical molecular self-assembly, and in turn producing well-defined submicrospheres. Spectroscopic analyses such as FE-SEM, TEM, DLS, NMR, XRD, and IR absorption spectroscopy indicates that the particles are composed of lamellar structures of sp^2 -hybridized trigonal planar poly(dioxaborole). The spontaneous self-organization is ascribable to reactive layer-by-layer assembly through sequential boronate esterification of the diboronic acid and the tetrahydroxybenzene whereby initially formed oligo(dioxaborole) may provide a platform for further reactions, thus resulting in the production of submicro-

spheres. It is interesting to note that the dynamic covalent functionality as a result of the dioxaborole linkage induced a stimuli-responsive change in morphology by not only a pH switch but also the exchange reaction with pentaerythritol. Further, a selective saccharide-induced change in the submicrosphere morphology was observed through a simple exchange reaction of dynamic covalent boronate esters with saccharides in THF; the selective change in morphology is visually detected through the color change in the solution. These findings can provide a useful insight into the design of stimuli-responsive hierarchical architectures based on boron-containing dynamic covalent bond.

Introduction

Dynamic covalent chemistry^[1] is an effective approach for producing constitutional dynamics,^[2] wherein molecules are endowed with a thermodynamically reversible nature, thus facilitating self-control and self-correction. The use of boronic acid complexation with diols and their congeners, such as catechols, has great promise in developing reversible boron-containing multicomponent systems wherein the boronate ester linkage serves as the intercomponent bond of supramolecular architectures.^[3] The dynamic structure-directing potential has led to not only well-defined self-organization involving macrocycles,^[4] capsules,^[5] and gels^[6] but also reversible polymers^[7] and boronic-acid-attached polymers.^[8] In the field of material science, boronate-ester-linked periodic covalent organic frameworks (COFs) with two-dimensional (2D)^[9] and 3D^[10] porous crystals have been prepared. Moreover, boronic acids recognize the diol motif through boronate esterification; such boronic-acid-appended systems have been explored for use as sensing protocols for diol derivatives such as saccharides.^[11] Despite the superior properties of boronic acids as structure-directing functional groups in supramolecular chemistry, hierarchical 3D self-organization, formed by sequential boronate esterification, with a well-defined morphology and dynamic functionality are unprecedented.

Herein, we report for the first time well-defined submicrospheres arising from sequential boronate esterification of benzene-1,4-diboronic acid (1) with 1,2,4,5-tetrahydroxybenzene (2), wherein spontaneously provided well-defined submicrospheres in ambient conditions in the presence of pyridine (Figure 1). The result is of scientific significance because dehydration under conditions proposed by Rambo and Lavigne^[12] resulted in an agglomeration with an ill-defined morphology

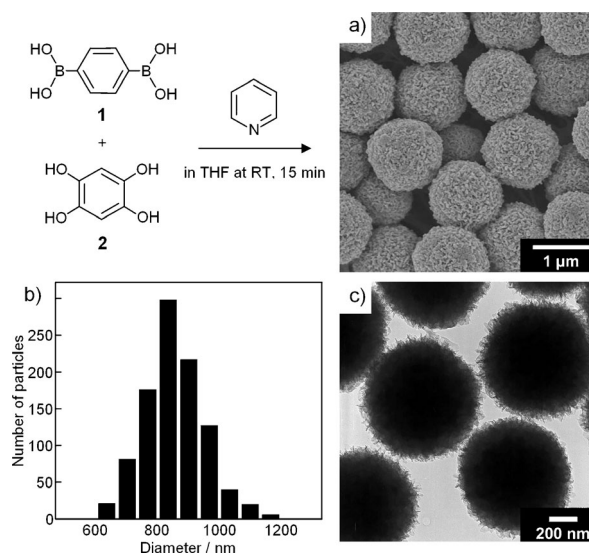


Figure 1. a) FE-SEM image of the submicrospheres formed by adding pyridine to a solution of 1 and 2 in THF. b) the size distribution of 1000 particles in the FE-SEM images. c) TEM image of the submicrospheres. Conditions: [1] = [2] = [pyridine] = 1.0×10^{-2} M in THF at room temperature. The resultant solids were isolated by filtration after 15 minutes reaction time.

[a] Dr. R. Nishiyabu, S. Teraoka, Y. Matsushima, Prof. Y. Kubo
Department of Applied Chemistry,
Graduate School of Urban Environmental Science,
Tokyo Metropolitan University
Minami-ohsawa, Hachioji, Tokyo 192-0397 (Japan)
Fax: (+81) 42-677-3134
E-mail: yujik@tmu.ac.jp

Supporting information for this article is available on the WWW under <http://dx.doi.org/10.1002/cplu.201100008>.

(see Figure S1 in the Supporting Information). A pyridine-catalyzed sequential boronate esterification enabled excellent morphology and dimensionality control of the hierarchical architectures by using chemical stimuli such as a pH switch and exchange reaction of the building blocks. Further, we demonstrate a selective saccharide-induced morphological change by taking advantage of the dynamic covalent functionalities of boronate esters; such an event is visually detectable through a color change in the solution.

Results and Discussion

The submicrospheres were easily obtained by the following procedure: to a solution of **1** (1.0×10^{-2} M) and **2** (1.0×10^{-2} M) in THF was added pyridine (1.0 equiv) to obtain a turbid suspension after 15 minutes. It is interesting to note that well-defined spherical particles were observed by field-emission scanning electron microscopy (FE-SEM; Figure 1a) and transmission electron microscopy (TEM; Figure 1c). Particle size distribution was taken from about 1000 particles observed in the FE-SEM images (see Figure S2); the histogram shows that the average diameter of the submicrospheres was 870 nm with a standard deviation of 100 nm (Figure 1b). These objects were formed in the solution; the size distribution was determined by dynamic light scattering (DLS) measurement (see Figure S3).

Analysis for components of the particles was carried out by using NMR spectroscopy. When the isolated solid was dissolved in $[D_6]DMSO$, the 1H NMR measurement exhibited singlet signals at 7.72 and 6.20 ppm, which were assigned to the aryl resonances of H^a and H^b , respectively (Figure 2a). The H^a

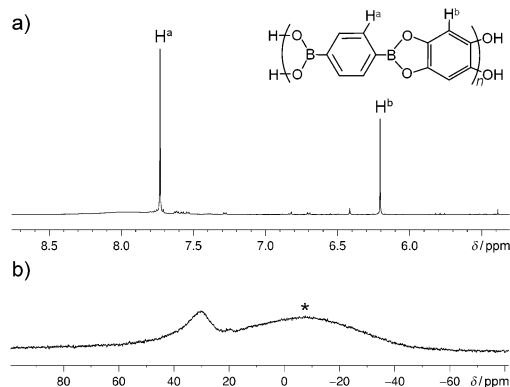


Figure 2. a) 1H and (b) ^{11}B NMR spectra of the submicrospheres dissolved in $[D_6]DMSO$ at 25 °C. A broad background peak (*) in the ^{11}B NMR spectrum is assigned to boron nitride used in the NMR probe.

signal was found to integrate in a 2:1 ratio with respect to that of H^b , thus implying that sequential boronate esterification occurred between **1** and **2**. Further assessment was made by ^{11}B NMR analysis in $[D_6]DMSO$ (Figure 2b) and a significant signal was observed at 30.04 ppm, which is indicative of the formation of sp^2 -hybridized trigonal planer boronate ester.^[13]

Boronate ester formation between **1** and **2** in the objects was also evidenced by infrared (IR) absorption spectroscopy with an attenuated total reflection (ATR) apparatus capable of avoiding the influence of water, wherein the disappearance of

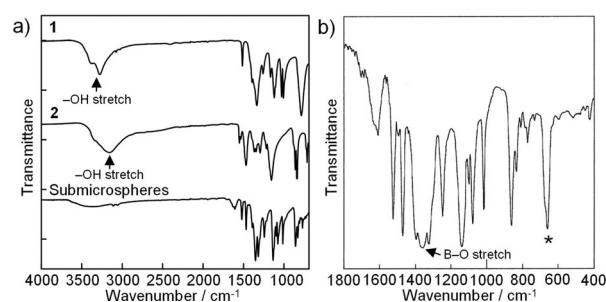


Figure 3. a) ATR-FT-IR spectra of **1**, **2**, and submicrospheres formed from **1** and **2**. b) IR spectrum (KBr method) of submicrospheres. A characteristic intense peak at 660 cm^{-1} (*) was assigned to boronate esters.

the $-OH$ stretching frequencies was observed at 3277 and 3147 cm^{-1} (Figure 3a). A characteristic intense signal assigned to boronate ester of **1** and **2** was also observed at 660 cm^{-1} together with a peak corresponding to $B-O$ stretch at 1359 cm^{-1} (Figure 3b; KBr method).^[12] Although it is known that coordination of pyridine to boron facilitates not only boronate esterification^[14] but also formation of boroxines^[15], the absence of a characteristic signal at near 580 cm^{-1} corresponding to boroxine structures indicates that boroxine structures were not formed under the reaction conditions we employed.

Powder X-ray diffraction (PXRD) analysis led us to analyze the nanostructures of the particles, which evinced the lamellar alignment of poly(dioxaborole)s in the submicrospheres (Figure 4a). The observed peaks at 25.5° and 27.4° corresponding to 3.49 and 3.25 \AA , which represent the distances between pol-

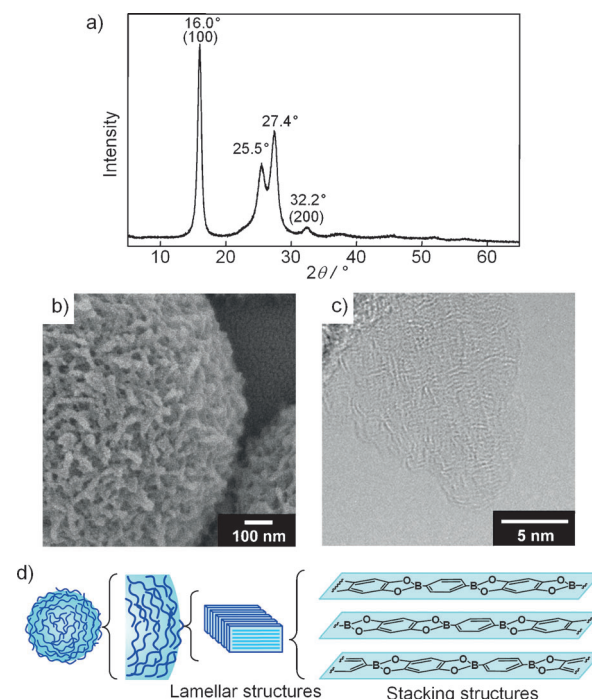


Figure 4. a) PXRD pattern of the submicrospheres. b) Observation of the surface of the submicrospheres by high-magnified FE-SEM and c) high-magnified TEM image of the surface. d) Plausible structures of the submicrosphere; lamellar structures composed of stacking structures of planar boronate ester polymers are self-assembled into the submicrosphere.

y(dioxaborole)s, and possibly result from interactions between the vacant pz orbital of boron and the π orbital. Diffraction peaks at 16.0° and 32.2° should represent lamellar packing of the stacked poly(dioxaborole)s in the submicrospheres (d -spacings of 5.53 Å). This packing leads to the production of a pyridine-free lamellar structure. Although this result was unexpected, the ^1H NMR spectrum of the spheres that were dissolved in $[\text{D}_6]\text{DMSO}$ exhibited a negligible amount of pyridine (Figure 2, see above); this led us to consider that the plausible reaction mechanism involves a conversion from pyridine-bound boronate ester polymer to pyridine-free planar boronate ester polymer (see below). From the PXRD data, one can estimate that approximately 10^9 dioxaborole units might be contained in the object having a diameter of 870 nm. Further assessment for the characterization came from a high-magnified FE-SEM image of the particles; the obtained particles were found to possess wrinkled nanostructures at the surface (Figure 4b). In addition, high-magnification TEM image on the edge of the condensed flake structures shows stripe patterns (Figure 4c), thus supporting the presence of nanostructures with a lamellar periodicity (estimated by PXRD). All these findings together indicate a plausible hierarchical supramolecular assembly of poly(dioxaborole)s, which is illustrated schematically in Figure 4d.

The reaction mechanism for the formation of submicrospheres is an intriguing subject that is explored in this study. This interest arises from the experiments carried out in THF at reflux and led to ill-defined fibrous agglomerates (see Figure S4). Initially, we focused on the role of pyridine because particle formation is initiated by adding pyridine into the solution of **1** and **2** in THF. An interaction between the boronic acid and an amino base, also known as a $\text{B}\cdots\text{N}$ interaction, lowered the $\text{p}K_{\text{a}}$ value of boronic acid, thus allowing boronate esterification to occur more easily than when under amine-free conditions.^[14] In fact, 2,6-di-*tert*-butylpyridine, which contained sterically hindered *tert*-butyl groups that prevents the $\text{B}\cdots\text{N}$ interaction, had a negligible effect on the solution (see Figure S5).

The Lewis basicity dependence of pyridines in particle formation was also investigated (Figure 5a–d). Although no reaction occurred in the presence of a weak base such as 3-cyanopyridine, the use of 3-picoline allowed us to detect well-defined and dispersed particles as seen in FE-SEM images and PXRD patterns, and is almost identical to the result obtained in the presence of pyridine. In contrast, on increasing the Lewis basicity of the pyridines, 4-methoxypyridine and 4-dimethylaminopyridine led to ill-defined shapes. The insight into the structure regulation came from ^1H NMR measurement of the solid derived with 4-dimethylaminopyridine (see Figure S6). When the solid species was dissolved in $[\text{D}_6]\text{DMSO}$ and then analyzed by using ^1H NMR spectroscopy, the signals corresponding to 4-dimethylaminopyridine appeared at 3.08, 6.83, and 8.15 ppm as well as signals arising from **1** and **2**, thus suggesting the production of 4-dimethylaminopyridine-containing species. It supports the observation that the pyridine-assisted particle formation involves a step in which the pyridine can be eliminated from the boronate ester. On the other hand, the use of triethylamine with a strong Brønsted base ($\text{p}K_{\text{a}}=10.8$)

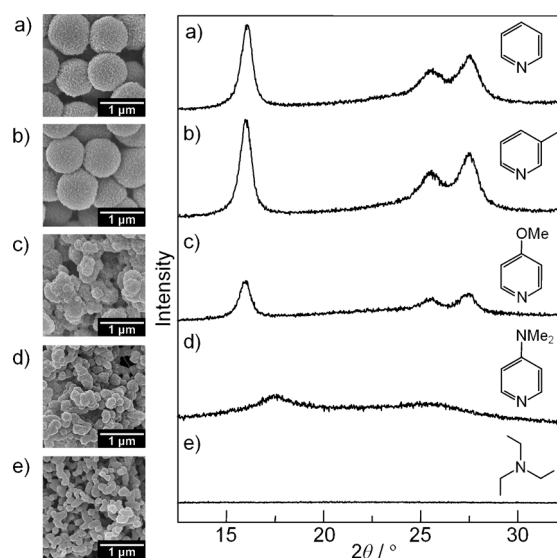


Figure 5. The basicity-dependence for the polymeric boronate esterification. The FE-SEM images and PXRD patterns of the solid isolated from the mixtures of **1** and **2** in THF at room temperature after the addition of (a) pyridine, (b) 3-picoline, (c) 4-methoxypyridine, (d) 4-dimethylaminopyridine, and (e) triethylamine, respectively. The use of 3-cyanopyridine induced no aggregation. Reaction conditions: $[\mathbf{1}] = [\mathbf{2}] = [\text{base}] = 1.0 \times 10^{-2}$ M. The solids were isolated from the mixture by filtration after 15 minutes reaction time.

resulted in agglomeration with no PXRD pattern (Figure 5e). The ^1H NMR spectra of the solid, being dissolved in $[\text{D}_6]\text{DMSO}$ (see Figure S7), exhibited signals at 1.17 (CH_2) and 3.08 ppm (CH_3) corresponding to the Et_3NH^+ ion. We thus reasoned that Et_3N could cause a deprotonation of **2** to assist boronate esterification of **1** and **2**. From these results, while an interaction of pyridine with boronic acid part is significant to cause sequential boronate esterification to form well-defined submicrospheres, thereby a strong interaction as well as strong base led to an agglomeration.

We also found that the particle dispersity was sensitively affected by the nature of the bulk solvent employed (Figure 6). When we used 1,4-dioxane ($E_{\text{T}}(30)=36.0$), which has a lower

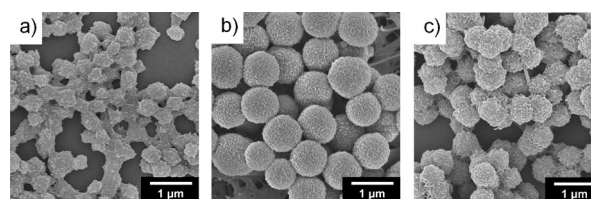


Figure 6. Morphology of the isolated solids formed in (a) 1,4-dioxane (b) THF, and (c) acetone. The $E_{\text{T}}(30)$ values of 1,4-dioxane, THF, and acetone are 36.0, 37.4, and 42.2, respectively. Reaction conditions: $[\mathbf{1}] = [\mathbf{2}] = [\text{pyridine}] = 1.0 \times 10^{-2}$ M at room temperature after 15 minutes reaction time.

polarity than THF ($E_{\text{T}}(30)=37.2$), partially agglomerated spheres were obtained, thus indicating that the morphology is sensitive to the bulk solvent. The solvophobic effect caused the integration of layers arising from polymeric boronate esterification. However, the use of solvent with a higher polari-

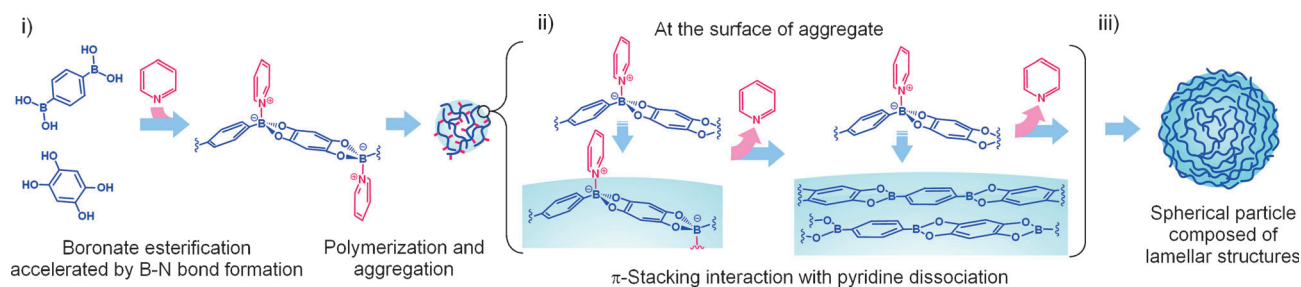


Figure 7. Schematic illustration of a plausible mechanism for the formation of the submicrospheres by reactive layer-by-layer assembly.

ty such as acetone ($E_T(30)=42.2$) resulted in agglomeration, and is possibly due to the enhanced interfacial free energy between the aggregation and the bulk solvent. In addition, there was no precipitate in DMSO ($E_T(30)=45.0$) involving **1**, **2**, and pyridine, thus indicating that good solvents for bis(dioxaborole)s do not induce particle formation.

From all these observations, we propose a plausible mechanism for the formation of the submicrospheres (Figure 7). This mechanism is based on the reactive layer-by-layer assembly of boronate ester-based polymers. It involves 1) coordination of pyridine to **1** thereby promoting polymeric boronate esterification with **2** to induce particle nucleation in the early stage, and 2) the initially formed spherical aggregates serving as a self-template for further boronate esterification, whereby pyridine-coordinated boronate ester oligomers/polymers are converted into planar structures via the elimination of pyridine, which is interpreted as the planar state that is composed of trigonal planar boronate ester, which is more thermodynamically favorable than the pyridine-coordinated tetrahedral structure because of interactions such as phenyl–boron–phenyl π stacking. Finally, the resulting polymers are spherical, which allows formation for minimization of the interfacial free energy between the particles and solvent used.^[16] Our proposed reactive layer-by-layer assembly is supported by the growth of the particles as a function of time, as indicated by the FE-SEM images (Figure 8). Note that small particles were produced after 30 second after aging of **1** and **2** in the presence of pyridine (Figure 8a). Time-dependent growth of the particles with well-defined morphology may be ascribable to solvophobic phenyl–boron–phenyl π -stacking interactions between poly(dioxaborole)s, thus resulting in the production of submicrospheres composed of denser flakes (Figure 8c).

The dynamic covalent functionality of boronate ester linkages in the particles drove us to investigate how the well-defined

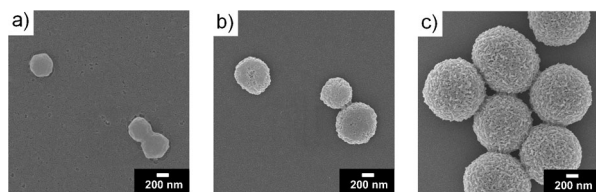


Figure 8. The FE-SEM images of submicrospheres at varied reaction times (a) 30 sec, (b) 1 min, and (c) 10 min. Reaction conditions: $[1] = [2] = [\text{pyridine}] = 1.0 \times 10^{-2} \text{ M}$ in THF at room temperature.

morphology would be affected by a pH switch in the solution (Figure 9). The addition of concentrated hydrochloric acid into a suspension of the isolated spheres in THF (Figure 9a) led to a clear solution in 24 hours (Figure 9b). The negligible scattering in the DLS measurement of the resulting solution indicated degradation of the submicroparticles based on cleavage of boronate ester linkages under acidic conditions.^[17] A lack of particle formation was still observed after the solution underwent neutralization with anhydrous sodium sulfate and dehydration with molecular sieve 4 Å (Figure 9c). However, subsequent addition of pyridine made the solution turbid again (Figure 9d). The DLS measurement of the solution showed strong light scattering, thus declaring the presence of colloidal particles. From the number size distribution and the intensity size distribution, the average diameter of the particles were determined to be $(823.6 \pm 179.7) \text{ nm}$ and $(1147.2 \pm 261.5) \text{ nm}$, respectively (see Figure S8). The FE-SEM image of the isolated solid allowed us to detect submicrospheres whose size and morphology was similar to that of the particles before degradation (Figure 9d, also see Figure S9). This outcome means that pyridine serves as a catalyst for the particle formation. In this manner, the reversible formation of submicrospheres was completed, thus leading to a system that is capable of self-assembly in response to changes in pH value.

It was anticipated that the exchange reaction, having multifunctional diols on the boronate ester linkages, would induce a change in morphology; we added pentaerythritol to a suspension of submicrospheres of **1** and **2** in THF at room temperature (Figure 10a). As a result, a slight change in the surface morphology was observed after three days (Figure 10c). Furthermore, after a few weeks the submicrospheres were finally transformed into particles composed of larger and sparser flakes (Figure 10e).

The transformation was attributed to the replacement of **2** with pentaerythritol in the polymeric structures as inferred from time-dependent PXRD patterns of the isolated solids at different reaction times (Figure 11). In the PXRD patterns, peaks at 16.0 , 25.5 and 27.6° corresponding to the packing structures of poly(dioxaborole)s of **1** and **2** (Figure 11a) decreased in the early stage (Figure 11b,c). Furthermore, four new peaks at 16.8 , 20.3 , 26.1 and 30.0° appeared in the course of the morphological changes (Figure 11d,e), thus indicating that the resultant flake structures possesses different components and packing structures from the original submicrospheres. In fact, boronate ester polymers separately prepared

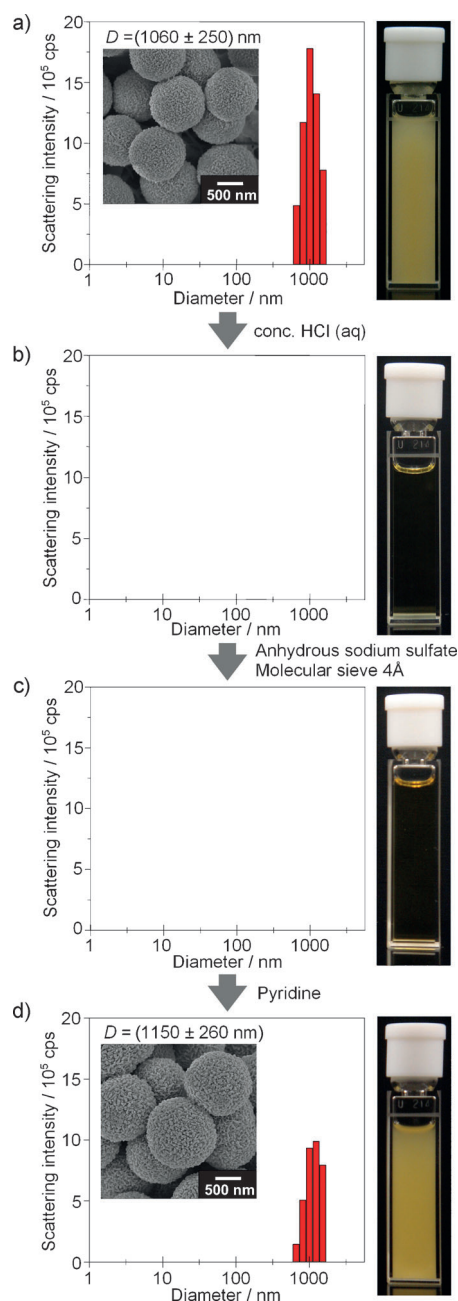


Figure 9. Intensity size distributions from DLS spectra for pH-triggered reversible formation of the submicrospheres. a) THF suspension of the submicrospheres, (b) after the addition of concentrated hydrochloric acid, (c) subsequent addition of anhydrous sodium sulfate and molecular sieve, and then (d) pyridine addition. The total scattering intensities of samples for (a), (b), (c), and (d) were 7.42×10^6 , 4.24×10^4 , 2.63×10^4 , and 7.91×10^6 cps, respectively.

from **1** and pentaerythritol in THF exhibit a similar diffraction pattern ($2\theta = 18.9, 21.0, 25.0,$ and 30.0° in Figure 11 f) with that of the final products of flake structures. The ^1H NMR spectrum of the polymer measured after 22 days, dissolved in D_2O , revealed approximately 80% of **2** was replaced by pentaerythritol (see Figure S10). This result strongly indicates that reversible boronate esterification enables us to control the self-assembly of the objects, thus leading to changes in the morphology.

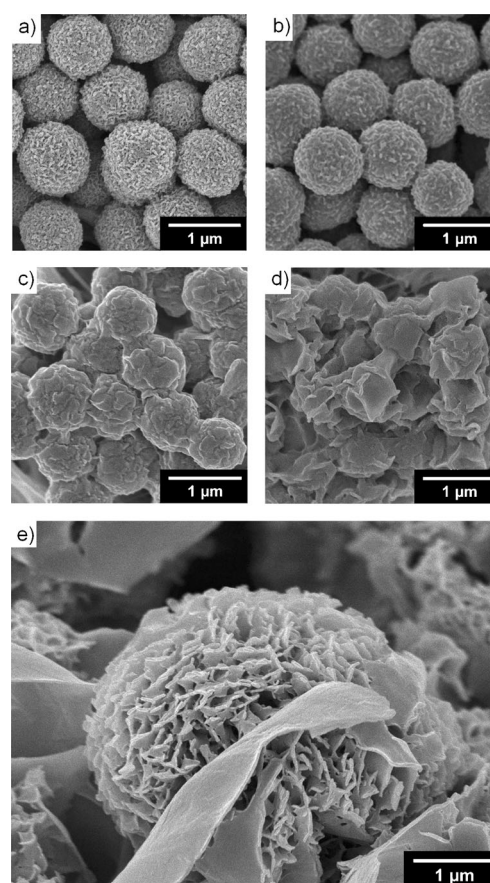


Figure 10. Morphological transformation of the submicrospheres based on constitutional dynamic functionality of boronate ester linkages. The FE-SEM images of the submicrospheres of **1** and **2** (12.0 mg, $0.051 \text{ mmol}^{[18]}$) upon the addition of pentaerythritol (6.0 mg, 0.044 mmol) in THF (4.0 mL) at different reaction times (before adding pentaerythritol (a), and 1 day (b), 3 days (c), 12 days (d), and 22 days (e) after adding pentaerythritol, respectively).

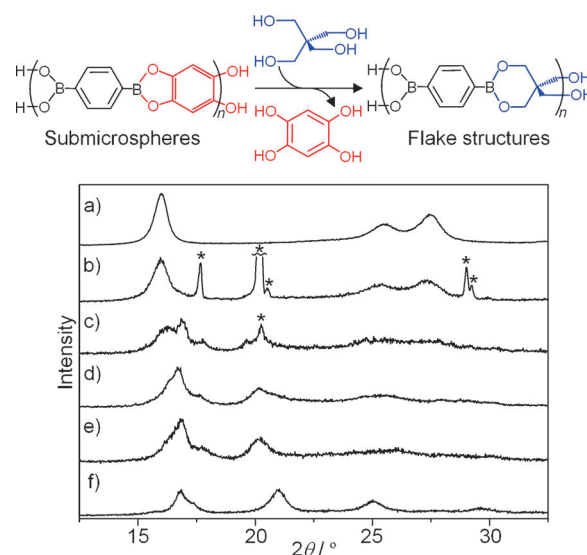


Figure 11. The XRD patterns of the submicrospheres of **1** and **2** (12.0 mg, $51.0 \text{ } \mu\text{mol}^{[18]}$) in THF for different reaction times (before adding pentaerythritol (a), and 1 day (b), 3 days (c), 12 days (d), and 22 days (e) after adding pentaerythritol (6.0 mg, $44.0 \text{ } \mu\text{mol}^{[18]}$), respectively) and boronate ester polymers obtained from **1** and pentaerythritol in THF (f). Peaks marked with asterisks are assigned to insoluble residue of pentaerythritol.

Next, our interest turned to finding out whether the submicrospheres would have a morphological signaling capability toward saccharides. This proposition is based on boronic acid–saccharide covalent interactions that readily occur in a solution.^[19] With this in mind, we separately added three kinds of saccharides, phenyl- β -D-galactopyranoside (**pGal**), phenyl- β -D-glucopyranoside (**pGlc**), and phenyl- β -D-xylopyranoside (**pXyl**), to the dispersed THF solutions containing the submicrospheres and aged these solutions for five days (Figure 12). Interestingly, fibrous aggregates were observed in the FE-SEM images when **pGal** was added, whereas the addition of **pGlc** or **pXyl** induced almost no morphological change. As a control experiment, when **pGal** was added to a solution of **1** in THF in the absence of **2**, similar fiberlike structures were obtained (see Figure S11). This outcome strongly suggests that the morphological changes from spherical to fiberlike structures upon the addition of **pGal** may be caused by the exchange reaction of building blocks between **2** and **pGal**.

The characterization of the fiberlike structures was evident from the ^1H NMR measurements; fibrous aggregates obtained from the reaction of the submicrospheres with **pGal** were dissolved in $[\text{D}_6]\text{DMSO}$. Subsequently, the ^1H NMR and ^1H – ^1H NOESY spectra indicate the production of the $(\text{pGal})_2\cdot(1)$ complex with a six-membered ring formed from a *cis*-CH(OH)-

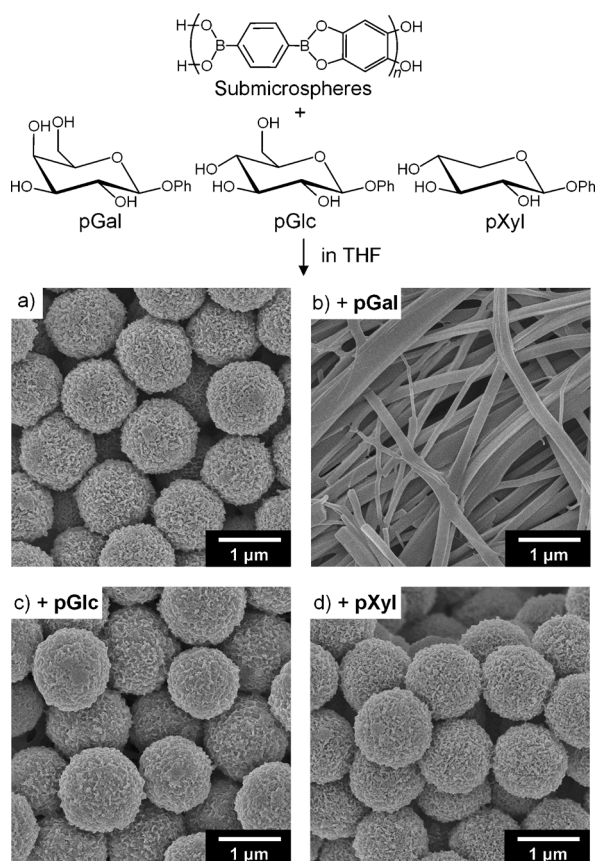


Figure 12. Influence on the morphology of the submicrospheres (2.0 mg, 8.5 μmol ^[18]): (a) saccharide-free condition, (b) **pGal** (22.0 mg, 85.0 μmol) addition, (c) **pGlc** (22.0 mg, 85.0 μmol) addition, and (d) **pXyl** (19.0 mg, 85.0 μmol) addition in THF (2.0 mL) at room temperature for five days.

CH(CH₂OH) and diol groups (Figure 13a, also see Figure S12). On the other hand, as shown in Figure 13b, the ^1H NMR spectrum of the particles isolated from the corresponding solution with **pGlc** was the same as that of the above-mentioned submicrospheres (Figure 2a). Such higher reactivity with **pGal**

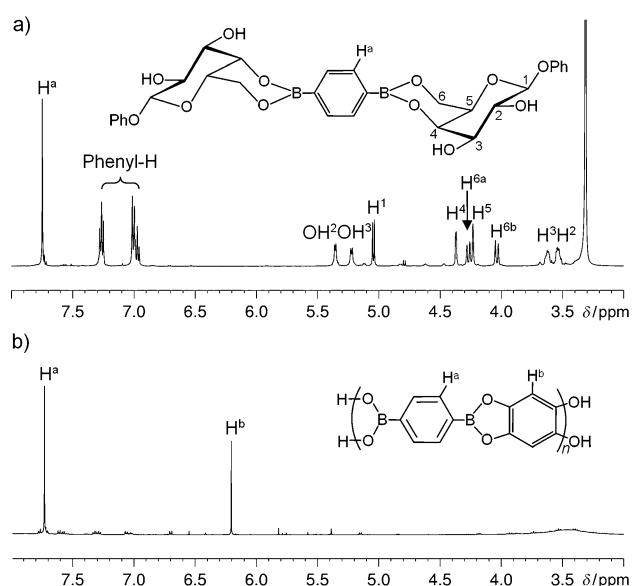


Figure 13. The ^1H NMR spectra of (a) the fibrous aggregates and (b) the particles in $[\text{D}_6]\text{DMSO}$, which were isolated after aging with **pGal** and **pGlc** at room temperature for five days, respectively.

compared to that with **pGlc** is consistent with the binding strength of phenylboronic acid with these saccharides,^[19] thus suggesting that the submicrospheres could selectively react with the saccharides.

Another interesting point is that after removing (by filtration) the fibrous aggregates composed of the $(\text{pGal})_2\cdot(1)$ complex, the resultant solution was orange and showed an absorption band at 388 nm. The ^1H NMR spectrum in $[\text{D}_6]\text{DMSO}$ clearly indicates a singlet signal at 5.82 ppm, which arises from the formation of 1,4-dihydroxy-*p*-benzoquinone (see Figure S13) and is probably the oxidized product of **2** eliminated from the particle by an exchange reaction with saccharide. Figure 14a shows the absorption spectra of the submicrospheres-dispersed THF solution in the presence of 10 equivalents of **pGal**; the absorption band at 388 nm gradually increased as a function of time. As inferred from Figure 14b, a specific response towards **pGal** was obtained because other saccharides tested here induced almost no change in the absorption spectra. This result strongly suggests that the saccharide-induced morphological signaling of the particles can be translated into a color change in the solution (see Figure S14).

Conclusion

In conclusion, we have developed a simple method for fabricating poly(dioxaborole) hierarchical soft particles by reactive layer-by-layer assembly through sequential boronate esterifica-

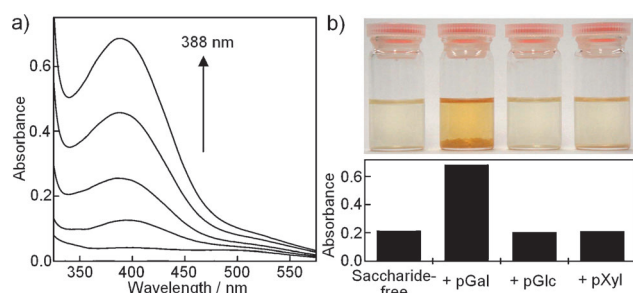


Figure 14. a) Absorption spectra of supernatant solution of submicrospheres (4.0 mg, $17.0 \mu\text{mol}$) dispersed in THF (4.0 mL) in the presence of 10 equivalents of **pGal**. Time-dependent absorption spectra were recorded (1, 2, 3, 4, and 5 day). b) Absorption intensity at 388 nm of supernatant solution of submicrospheres (4.0 mg; $17.0 \mu\text{mol}$) dispersed in THF (4.0 mL) in the presence of 10 equivalents of **pGal**, **pGlc**, and **pXyl**, respectively. The data were collected after aging the solution at room temperature for five days.

tion. By taking advantage of boron-based dynamic covalent functionality, we demonstrated not only the reversible formation of the particles on pH switching but also the transformation in morphology using pentaerythritol. Furthermore, the fact that the particles have a morphological signaling capability toward saccharides is noteworthy; the recognition event can be detected by the naked eye owing to the production of 1,4-dihydroxy-*p*-benzoquinone in the solution. The ready availability of boronic acids and catechols/diols allowed us to prepare a variety of chemical stimuli-responsive 3D soft systems. Additionally, the surface of this material is composed of Lewis acidic sp^2 -hybridized trigonal planar boronate ester, which opens up new possibilities for the use of scaffold entities in various application fields that involve organic/inorganic hybrid materials, polymer-supported catalysts, sensor particles, and separation media. Further research in this regard is currently underway in our laboratory.

Experimental Section

General procedures

Field-emission scanning electron microscopy (FE-SEM) and transmission electron microscopy (TEM) were performed by JEOL JSM-7500F (acceleration voltage of 5 kV), JEOL JEM-2000FX (acceleration voltage of 200 kV), and JEOL JEM-3200FS (acceleration voltage of 300 kV) electron microscopes, respectively. For FE-SEM measurements, submicrospheres were collected on a PTFE membrane filter (pore size of 0.1 μm ; Advantec Toyo Kaisha, Ltd.) by filtration or on a glass substrate by casting of the suspensions. These samples were coated with Au on an EIKO IB3 ION COATER. For TEM measurements, a suspension of submicrospheres in THF was placed on a carbon-meshed copper grid (Elastic carbon substrate on STEM100Cu grids; Okenshoji Co., Ltd.) and the solution was immediately filtered by using a filtration paper. The resultant grid was dried in vacuum and measured without staining. Determination of average diameters of the submicrospheres from FE-SEM was calculated from the 1000 particles in the FE-SEM images. Dynamic light scattering (DLS) was measured using an Otsuka Electronic ELSZ-2. The scattering angle of the apparatus is 165.7° to collect light scattering from near the surface of a sample cell. The values of viscosity (0.5505 cp), refractive index (1.4000) of THF were used. Hydrody-

namic radius was calculated from Stokes-Einstein relationship with the cumulant method. Intensity size distributions of the submicrospheres were calculated by the Marquardt method. The infrared spectrum of the submicrospheres was recorded on a JASCO FT/IR-5300 spectrometer by using the KBr pellet technique. To detect peaks corresponding to OH stretch of **1**, **2**, and the submicrospheres, the infrared spectra were measured with a SHIMADZU IRAffinity-1 equipped with an attenuated total reflection (ATR) apparatus. The ^1H , ^{11}B , and ^1H - ^1H NOESY NMR spectra were recorded on a Bruker AVANCE-500 spectrometer using tetramethylsilane (TMS) as internal standard (0 ppm) for ^1H NMR analysis and $\text{BF}_3\text{-OEt}_2$ as an external standard (0 ppm) for ^{11}B NMR analysis. All spectra were recorded at 298 K. Powder X-ray diffraction (PXRD) data were collected by Rigaku RINT-TTR III X-ray diffractometer with $\text{Cu K}\alpha$ radiation. Absorption spectra were obtained on Shimadzu UV-3100PC spectrophotometer at 25°C and a quartz cell with 1 cm path length was used.

Materials

Synthesis of 1,2,4,5-tetrahydroxybenzene (**2**) was performed according to the literature as follows:^[12,20] A suspension of 2,5-dihydroxy-1,4-benzoquinone (10.7 g, 76.7 mmol) and granular tin (10.9 g) in concentrated hydrochloric acid (233 mL) was heated at reflux in a 500 mL round-bottom flask equipped with a condenser. After 1 h, the granular tin was removed by passage through a glass filter and the reaction mixture was cooled to room temperature. The resultant brown needle crystal was collected and recrystallization from THF twice afforded white platelike crystals (7.4 g, 68% yield). ^1H NMR (500 MHz, $[\text{D}_6]\text{DMSO}$, TMS): $\delta = 6.20$ (s, 2H; Ar-H), 7.94 (s, 4H; OH). THF was distilled from sodium wire with benzophenone before use. All other reagents were purchased from commercial suppliers and used without further purification.

Preparation of submicrospheres

Benzene-1,4-diboronic acid (**1**, 16.6 mg, 0.10 mmol) and **2** (14.2 mg, 0.10 mmol) were dissolved in freshly distilled THF (5 mL), respectively. To a mixture of the THF solutions was added pyridine (7.9 μL , 0.10 mmol). The resultant mixture was then allowed to stand for 15 min at RT. In this period, the reaction mixture became a turbid suspension. The resultant solids were isolated by filtration and used for further study (yield = 18.4 mg). In the experiments for the effect of steric hindrance and basicity-dependence of bases on the polymeric boronate esterification, 2,6-di-*tert*-butylpyridine, 3-cyanopyridine, 3-picoline, 4-methoxypyridine, 4-dimethylaminopyridine, and triethylamine were used. To solutions of **1** (0.10 mmol) and **2** (0.10 mmol) in THF (10 mL) were separately added pyridine derivatives (0.10 mmol) and then the reaction mixtures were allowed to stand for 15 min at RT. The solids formed by the addition of 3-picoline, 4-methoxypyridine, 4-dimethylaminopyridine and triethylamine were collected by filtration for SEM and PXRD experiments. For the study on the effect of solvent on the particle dispersity, boronate esterification was performed using 1,4-dioxane, acetone, and DMSO in the same manner.

pH-Triggered reversible formation

To a suspension of submicrospheres (70.0 mg) in THF (30 mL) was added concentrated hydrochloric acid (0.22 mL). The resultant mixture was allowed to stand at RT for 24 h until the solution became clear. Degradation of submicrospheres into component monomers

was confirmed by DLS measurement of the resultant clear solution. The degraded solution was dehydrated with anhydrous sodium sulfate and molecular sieve (4 Å) in a freezer for 12 h. To the dehydrated solution (2.5 mL) was added pyridine (2.0 µL). The resultant mixture became turbid within minutes and the solids were isolated by filtration for SEM observation.

Morphological transformation of submicrospheres

To a suspension of submicrospheres (12.0 mg, 51.0 µmol^[18]) in THF (4.0 mL) was added pentaerythritol (6.0 mg, 44.0 µmol) and the resultant mixture was allowed to stand at RT. The solids were isolated by filtration at varied reaction times for SEM and PXRD experiments. In the experiments using sugars as chemical stimuli, phenyl-β-D-galactopyranoside (22.0 mg, 85.0 µmol), phenyl-β-D-glucopyranoside (22.0 mg, 85.0 µmol); and phenyl-β-D-xylopyranoside (19.0 mg, 85.0 µmol) were separately added to the submicrospheres (2.0 mg, 8.5 µmol^[18]) in THF (2.0 mL), respectively. The mixtures were allowed to stand at RT for five days and the solids were collected on PTFE membrane filters by filtration for NMR and SEM studies of the products.

Acknowledgements

This research was supported by a Grant-in-Aid for Scientific Research from the Ministry of Education, Science, Sports and Culture of Japan (grant nos. 21550137, 23750167) and the Yamada Science Foundation.

Keywords: boron • dynamic covalent chemistry • nanostructures • self-assembly • supramolecular chemistry

- [1] a) S. J. Rowan, S. J. Cantrill, G. R. L. Cousins, J. K. M. Sanders, J. F. Stoddart, *Angew. Chem.* **2002**, *114*, 938–993; *Angew. Chem. Int. Ed.* **2002**, *41*, 898–952; b) P. T. Corbett, J. Leclair, L. Vial, K. R. West, J.-L. Wietor, J. K. M. Sanders, S. Otto, *Chem. Rev.* **2006**, *106*, 3652–3711; c) I. Huc, J.-M. Lehn, *Proc. Natl. Acad. Sci. USA* **1997**, *94*, 2106–2110; d) J.-M. Lehn, *Chem. Eur. J.* **1999**, *5*, 2455–2463; e) J.-M. Lehn, *Proc. Natl. Acad. Sci. USA* **2002**, *99*, 4763–4768; f) J.-M. Lehn, *Science* **2002**, *295*, 2400–2403; g) O. Ramström, J.-M. Lehn, *Nat. Rev. Drug Discovery* **2002**, *1*, 26–36; h) K. Severin, *Chem. Eur. J.* **2004**, *10*, 2565–2580.
- [2] J.-M. Lehn, *Chem. Soc. Rev.* **2007**, *36*, 151–160.
- [3] a) N. Fujita, S. Shinkai, T. D. James, *Chem. Asian J.* **2008**, *3*, 1076–1091; b) K. Severin, *Dalton Trans.* **2009**, 5254–5264; c) A. L. Korich, P. M. Iovine, *Dalton Trans.* **2010**, *39*, 1423–1431; d) F. Jäkle, *Chem. Rev.* **2010**, *110*, 3985–4022; e) R. Nishiyabu, Y. Kubo, T. D. James, J. S. Fossey, *Chem. Commun.* **2011**, *47*, 1124–1150.
- [4] a) V. Barba, R. Villamil, R. Luna, C. Godoy-Alcántara, H. Höpfl, H. I. Beltran, L. S. Zamudio-Rivera, R. Santillan, N. Farfán, *Inorg. Chem.* **2006**, *45*, 2553–2561; b) N. Christinat, R. Scopelliti, K. Severin, *J. Org. Chem.* **2007**, *72*, 2192–2200; c) N. Iwasawa, H. Takahagi, *J. Am. Chem. Soc.* **2007**, *129*, 7754–7755; d) H. Takahagi, N. Iwasawa, *Chem. Eur. J.* **2010**, *16*, 13680–13688.
- [5] a) K. Kataoka, S. Okuyama, T. Minami, T. D. James, Y. Kubo, *Chem. Commun.* **2009**, 1682–1684; b) K. Kataoka, T. D. James, Y. Kubo, *J. Am. Chem. Soc.* **2007**, *129*, 15126–15127; c) N. Nishimura, K. Kobayashi, *J. Org. Chem.* **2010**, *75*, 6079–6085; d) N. Nishimura, K. Yoza, K. Kobayashi, *J. Am. Chem. Soc.* **2010**, *132*, 777–790; e) N. Nishimura, K. Kobayashi, *Angew. Chem.* **2008**, *120*, 6351–6354, *Angew. Chem. Int. Ed.* **2008**, *47*, 6255–6258.
- [6] a) Y. Kubo, W. Yoshizumi, T. Minami, *Chem. Lett.* **2008**, *37*, 1238–1239; b) L. He, D. E. Fullenkamp, J. G. Rivera, P. B. Messersmith, *Chem. Commun.* **2011**, *47*, 7497–7499.
- [7] a) I. Nakazawa, S. Suda, M. Masuda, M. Asai, T. Shimizu, *Chem. Commun.* **2000**, 881–882; b) W. Niu, C. O'Sullivan, B. M. Rambo, M. D. Smith, J. J. Lavigne, *Chem. Commun.* **2005**, 4342–4344.
- [8] a) T. Nagasaki, T. Kimura, S. Arimori, S. Shinkai, *Chem. Lett.* **1994**, 1495–1498; b) H. Kobayashi, M. Amai, J. H. Jung, A. Friggeri, S. Shinkai, D. N. Reinhoudt, *Chem. Commun.* **2001**, 1038–1039; c) H. Kobayashi, K. Koumoto, J. H. Jung, S. Shinkai, *J. Chem. Soc. Perkin Trans. 2* **2002**, 1930–1936; d) Y. Qin, V. Sukul, D. Pagakos, C. Cui, F. Jäkle, *Macromolecules* **2005**, *38*, 8987–8990; e) J. N. Cambre, D. Roy, S. R. Gondi, B. S. Sumerlin, *J. Am. Chem. Soc.* **2007**, *129*, 10348–10349; f) D. Roy, J. N. Cambre, B. S. Sumerlin, *Chem. Commun.* **2008**, 2477–2479; g) D. Roy, J. N. Cambre, B. S. Sumerlin, *Chem. Commun.* **2009**, 2106–2108; h) P. De, S. R. Gondi, D. R. B. S. Sumerlin, *Macromolecules* **2009**, *42*, 5614–5621; i) C. Cui, E. M. Bonder, Y. Qin, F. Jäkle, *J. Polym. Sci. A: Polym. Chem.* **2010**, *48*, 2438–2445; j) F. Cheng, F. Jäkle, *Polym. Chem.* **2011**, *2*, 2122–2132.
- [9] a) A. P. Côté, A. I. Benin, N. W. Ockwig, M. O'Keeffe, A. J. Matzger, O. M. Yaghi, *Science* **2005**, *310*, 1166–1170; b) R. W. Tilford, W. R. Gemmill, H.-C. zur Loye, J. J. Lavigne, *Chem. Mater.* **2006**, *18*, 5296–5301; c) A. P. Côté, H. M. El-Kaderi, H. Furukawa, J. R. Hunt, O. M. Yaghi, *J. Am. Chem. Soc.* **2007**, *129*, 12914–12915; d) R. W. Tilford, S. J. Mugavero III, P. J. Pellechia, J. J. Lavigne, *Adv. Mater.* **2008**, *20*, 2741–2746; e) S. Wan, J. Guo, J. Kim, H. Ihee, D. Jiang, *Angew. Chem.* **2008**, *120*, 8958–8962; *Angew. Chem. Int. Ed.* **2008**, *47*, 8826–8830; f) S. S. Han, H. Furukawa, O. M. Yaghi, W. A. Goddard, *J. Am. Chem. Soc.* **2008**, *130*, 11580–11581; g) N. L. Campbell, R. Clowes, L. K. Ritchie, A. I. Cooper, *Chem. Mater.* **2009**, *21*, 204–206; h) S. Wan, J. Guo, J. Kim, H. Ihee, D. Jiang, *Angew. Chem.* **2009**, *121*, 5547–5550; *Angew. Chem. Int. Ed.* **2009**, *48*, 5439–5442; i) C. J. Doonan, D. J. Tranchemontagne, T. Grant Glover, J. R. Hunt, O. M. Yaghi, *Nat. Chem.* **2010**, *2*, 235–238; j) E. L. Spitler, W. R. Dichtel, *Nat. Chem.* **2010**, *2*, 672–677; k) J. W. Colson, A. R. Woll, A. Mukherjee, M. P. Levendorf, E. L. Spitler, V. B. Shields, M. G. Spencer, J. N. W. R. Dichtel, *Science* **2011**, *332*, 228–231; l) X. Feng, L. Chen, Y. Dong, D. Jiang, *Chem. Br. Chem. Commun.* **2011**, *47*, 1979–1981; m) X. Ding, J. Guo, X. Feng, Y. Honsho, J. Guo, S. Seki, P. Maitarad, A. Saeki, S. Nagase, D. Jiang, *Angew. Chem.* **2011**, *123*, 1325–1329; *Angew. Chem. Int. Ed.* **2011**, *50*, 1289–1293; n) E. L. Spitler, M. R. Giovino, S. L. White, W. R. Dichtel, *Chem. Sci.* **2011**, *2*, 1588–1593; o) S. Wan, F. Gándara, A. Asano, H. Furukawa, A. Saeki, S. K. Dey, L. Liao, M. W. Ambrogio, Y. Y. Botros, X. Duan, S. Seki, J. F. Stoddart, O. M. Yaghi, *Chem. Mater.* **2011**, *23*, 4094–4097; p) L. M. Lanni, R. W. Tilford, M. Bharathy, J. J. Lavigne, *J. Am. Chem. Soc.* **2011**, *133*, 13975–13983; q) X. Ding, L. Chen, Y. Honsho, X. Feng, O. Saengsawang, J. Guo, A. Saeki, S. Seki, S. Irie, S. Nagase, V. Parasuk, D. Jiang, *J. Am. Chem. Soc.* **2011**, *133*, 14510–14513; r) E. L. Spitler, B. T. Koo, J. L. Novotney, J. W. Colson, F. J. Uribe-Romo, G. D. Gutierrez, P. Clancy, W. R. Dichtel, *J. Am. Chem. Soc.* **2011**, *133*, 19416–19421.
- [10] a) H. M. El-Kaderi, J. R. Hunt, J. L. Mendoza-Cortés, A. P. Côté, R. E. Taylor, M. O'Keeffe, O. M. Yaghi, *Science* **2007**, *316*, 268–272; b) H. Furukawa, O. M. Yaghi, *J. Am. Chem. Soc.* **2009**, *131*, 8875–8883; c) D. Cao, J. Lan, W. Wang, B. Smit, *Angew. Chem.* **2009**, *121*, 4824–4827; *Angew. Chem. Int. Ed.* **2009**, *48*, 4730–4733.
- [11] a) T. D. James, P. Linnane, S. Shinkai, *Chem. Commun.* **1996**, 281–288; b) T. D. James, S. Shinaki, *Top. Curr. Chem.* **2002**, *218*, 159–200; c) R. Nishiyabu, Y. Kubo, T. D. James, J. S. Fossey, *Chem. Commun.* **2011**, *47*, 1106–1123.
- [12] B. M. Rambo, J. J. Lavigne, *Chem. Mater.* **2007**, *19*, 3732–3739.
- [13] M. T. Reetz, C. M. Niemeyer, K. Harms, *Angew. Chem.* **1991**, *103*, 1515–1517; *Angew. Chem. Int. Ed. Engl.* **1991**, *30*, 1472–1474.
- [14] a) G. Wulff, M. Lauer, H. Böhnke, *Angew. Chem.* **1984**, *96*, 714–716; *Angew. Chem. Int. Ed. Engl.* **1984**, *23*, 741–742; b) M. Lauer, H. Böhnke, R. Grotstollen, M. Salehnia, G. Wulff, *Chem. Ber.* **1985**, *118*, 246–260; c) M. Lauer, G. Wulff, *J. Chem. Soc. Perkin Trans. 2* **1987**, 745–749; d) S. L. Wiskur, J. J. Lavigne, H. Ait-Haddou, V. Lynch, Y. H. Chiu, J. W. Canary, E. V. Anslyn, *Org. Lett.* **2001**, *3*, 1311–1314; e) L. Zhu, S. H. Shabbir, M. Gray, V. M. Lynch, S. Sorey, E. V. Anslyn, *J. Am. Chem. Soc.* **2006**, *128*, 1222–1232; f) E. Sheepwash, V. Krampl, R. Scopelliti, O. Sereda, A. Neels, K. Severin, *Angew. Chem.* **2011**, *123*, 3090–3093; *Angew. Chem. Int. Ed.* **2011**, *50*, 3034–3037.
- [15] a) J. Kua, M. N. Fletcher, P. M. Iovine, *J. Phys. Chem. A* **2006**, *110*, 8158–8166; b) J. Kua, P. M. Iovine, *J. Phys. Chem. A* **2005**, *109*, 8938–8943; c) E. K. Perltu, M. Arnold, P. M. Iovine, *Tetrahedron Lett.* **2005**, *46*, 8753–8756.

- [16] a) M. Oh, C. A. Mirkin, *Nature* **2005**, *438*, 651–654; b) T. Nakanishi, W. Schmitt, T. Michinobu, D. G. Kurth, K. Ariga, *Chem. Commun.* **2005**, 5982–5984; c) H. Maeda, M. Hasegawa, T. Hashimoto, T. Kakimoto, S. Nishio, T. Nakanishi, *J. Am. Chem. Soc.* **2006**, *128*, 10024–10025; d) Y. Su, Q. He, X. Yan, J. Fei, Y. Cui, J. Li, *Chem. Eur. J.* **2011**, *17*, 3370–3375.
- [17] G. Springsteen, B. Wang, *Tetrahedron* **2002**, *58*, 5291–5300.
- [18] The concentration was based on the monomer unit.
- [19] J. P. Lorand, J. O. Edwards, *J. Org. Chem.* **1959**, *24*, 769–774.
- [20] P. R. Weider, L. S. Hegedus, H. Asada, S. V. D'Andreq, *J. Org. Chem.* **1985**, *50*, 4276–4281.

Received: September 25, 2011

Revised: December 24, 2011

Published online on January 26, 2012